

## Two-Beam Modulation Instability in Noninstantaneous Nonlinear Media

I. Velchev, R. Pattnaik, and J. Toulouse

*Department of Physics, Lehigh University, 16 Memorial Drive East, Bethlehem, Pennsylvania 18015, USA*  
(Received 25 April 2003; published 29 August 2003)

The development of modulation instability for two beams copropagating in a medium with non-instantaneous nonlinear response is investigated. The frequency dependence of the experimentally observed spectral broadening reveals the presence of two-beam coupling, resulting from the time-delayed Raman part of the third-order nonlinear susceptibility. We present an analysis of the experimental data, which yields a value of  $\tau = 27(1)$  fs for the lifetime of the optical phonons in silica fibers. To our knowledge, this is the first experimentally determined value for this important material parameter.

DOI: 10.1103/PhysRevLett.91.093905

PACS numbers: 42.81.Dp, 42.65.Sf

The coupling between two optical waves in a nonlinear medium leads to a wide variety of fascinating effects. Distributed Raman amplification (DRA), four-wave mixing, and modulation instability (MI) are the most important ones with implications for the fiber communication systems. DRA offers high gain, high saturation power, fast response, and broad amplification bandwidth in an all-fiber device. All these features make it a particularly attractive amplification process for use in fiber communication systems. For a single optical wave, MI develops as a result of the interplay between self-phase modulation (SPM) and anomalous group velocity dispersion (GVD) [1]. It is the nonlinear effect responsible for the breakup of a continuous-wave (cw) beam into a train of ultrashort pulses [2], which also underlies the process of soliton formation in optical fibers. Its signature is the exponential growth of symmetrical sidebands around the central peak in the spectrum of the optical wave. Any perturbation on either the amplitude or the phase of the wave, at the frequency of the sidebands, will be amplified and will eventually lead to an instability. Broadband spontaneous Raman scattering can serve as an efficient noise source for the development of MI and is found to lead to soliton-Raman generation [3]. Cross-phase modulation (XPM) can contribute to MI in both normal and anomalous dispersion regimes [4,5] for two copropagating optical waves in a nonlinear medium. In this Letter, we analyze both theoretically and experimentally the relationship between MI and XPM in the presence of the delayed-response two-wave coupling [6] provided by the Raman scattering process in optical fibers. As a particular example, the development of two-beam MI in a cw Raman fiber amplifier is experimentally investigated.

A commercial Raman fiber laser (RFL) operating at 1497 nm with a spectral bandwidth  $\Delta\lambda \approx 1$  nm at 1.5 W maximum power is used as a pump source for DRA in an optical fiber. The signal source is a narrow-band external cavity diode laser, continuously tunable over a broad wavelength range (1450–1650 nm) and delivering maximum power of 3.2 mW. The pump and the signal waves

are launched into a single-mode fiber by means of a fiber coupler, and their spectra are recorded at the output by an optical spectrum analyzer. In our study, two types of commercially available optical fibers are used: Allwave and Truwave (Optical Fiber Solutions) [7]. Both Allwave (25 km) and Truwave (20 km) fibers have attenuation of  $\approx 0.22$  dB/km and respective mode-field areas:  $A_{\text{eff}} = 87 \mu\text{m}^2$  (Allwave) and  $A_{\text{eff}} = 55 \mu\text{m}^2$  (Truwave).

The experiment discussed is essentially of a pump-probe type in the frequency domain. A powerful cw pump at frequency  $\omega_1$  interacts, along the length of the optical fiber, with a weak cw probe beam tunable in frequency  $\omega_2$ . As a result of this interaction, the spectrum of the probe wave is modified through the interplay of the following processes: (i) Raman amplification; (ii) cross-phase modulation; (iii) GVD. Under certain conditions [4,5], MI sidebands appear on both sides of the probe carrier frequency, thus effectively broadening its spectrum.

In Allwave fiber, the broadened probe spectra are shown in Figs. 1(a)–1(c) with solid lines. They correspond to three different offsets from the pump frequency, respectively, on the red side [Fig. 1(a)], at the peak [Fig. 1(b)], and on the blue side [Fig. 1(c)] of the Raman gain curve. Our measurements show that the sidebands are always symmetrically positioned around the central signal frequency. The slight variation in their relative intensity is due to the Raman gain slope at each particular probe frequency, whereas their absolute intensity follows closely the Raman gain curve. In the following, the sideband with the lowest frequency is referred to as the red sideband and the highest frequency one as the blue sideband. The frequency difference between the sideband and the carrier frequency of the probe is referred to as the sideband frequency shift  $\Delta$ . For comparison, the spectra recorded in the Truwave fiber are shown with dashed lines in Figs. 1(a)–1(c), where no sidebands are observed. Such behavior is to be expected, considering the fact that the Truwave fiber exhibits small normal dispersion ( $\lambda_{\text{ZD}} = 1500$  nm) for the pump and anomalous dispersion

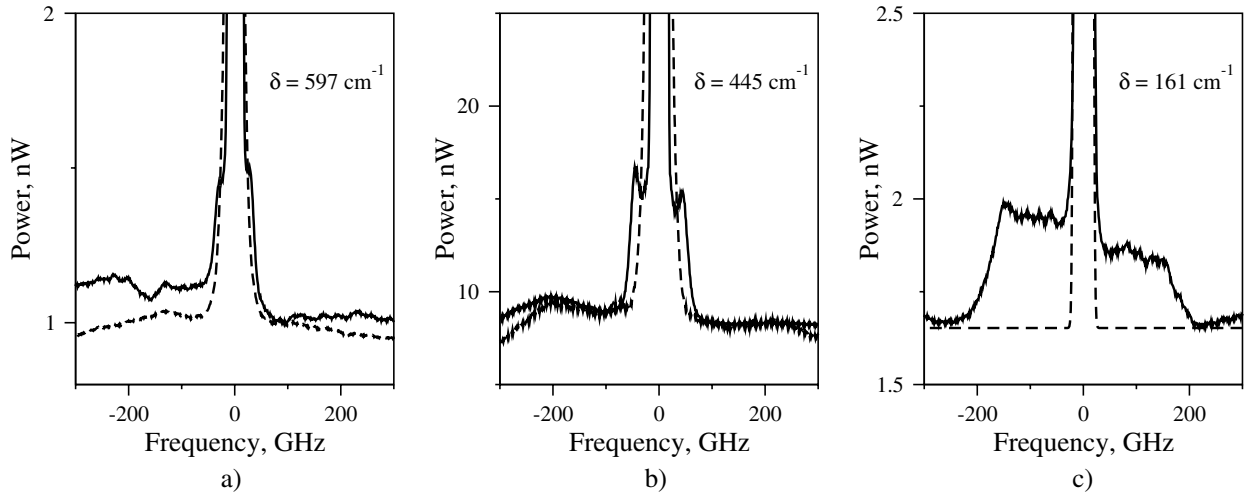


FIG. 1. Broadened spectra after Raman amplification in 25 km of Allwave fiber (solid line) for three probe frequency offsets: (a)  $\delta = 597 \text{ cm}^{-1}$ ; (b)  $\delta = 445 \text{ cm}^{-1}$ ; (c)  $\delta = 161 \text{ cm}^{-1}$ . The dashed lines represent the spectra from 20 km Truwave fiber under the same experimental conditions.

at the signal wavelength [7]; both SPM-induced MI for the pump wave and XPM-induced MI for the signal are therefore inhibited [4]. On the other hand, because the Allwave fiber exhibits anomalous dispersion at both pump and signal wavelengths, both SPM- and XPM-induced MI can develop. The same experiment with counterpropagating pump and signal beams shows no sidebands for both fibers.

In Figs. 1(a)–1(c), the sideband frequency shift  $\Delta$  is clearly seen to be larger, when the signal frequency approaches that of the pump ( $\delta \rightarrow 0$ ). This frequency dependence cannot be explained by the instantaneous interplay between GVD and XPM, as analyzed in Ref. [4]. In order to describe this effect, the finite response time  $\tau$  of the Kerr nonlinearity must be taken into account. In our theoretical treatment it is assumed that the third-order susceptibility can be split into two independent parts: an instantaneous electronic part and a time-delayed nuclear part. The former arises from nonresonant

virtual electronic transitions and has a characteristic time  $\tau_e$  of less than a femtosecond, whereas the latter is due mainly to the lifetime of nuclear vibrations  $\tau \sim 30 \text{ fs}$  [8]. The general form of the third-order susceptibility can be expressed as:

$$\chi^{(3)}(t) = \chi^{(3)}[(1 - \alpha)\delta(t) + \alpha g_R(t)], \quad (1)$$

where  $g_R(t)$  is the normalized Raman response function  $\int_0^\infty g_R(t)dt = 1$  and  $\alpha$  is the fractional contribution of the Raman part of the nonlinearity. From Raman scattering cross-section and gain measurements, this contribution is estimated to be  $\alpha \approx 0.18$  [9].

The coupled nonlinear evolution equations [10] for the slowly varying amplitudes of two plane waves with nonoverlapping spectra, centered around  $\omega_1$  (pump) and  $\omega_2 = \omega_1 - \delta$  (signal) and copropagating in a Kerr-type nonlinear medium, can be modified following the procedure described in Ref. [6], using the delayed-response nonlinearity from Eq. (1):

$$\frac{\partial}{\partial z} A_1 + \frac{1}{v_{g1}} \frac{\partial}{\partial t} A_1 = -i \left[ \frac{\beta_{21}}{2} \frac{\partial^2}{\partial t^2} - \gamma_1 (|A_1|^2 + \kappa(\delta) |A_2|^2) \right] A_1 - \gamma_1 \eta(\delta) |A_2|^2 A_1, \quad (2a)$$

$$\frac{\partial}{\partial z} A_2 + \frac{1}{v_{g2}} \frac{\partial}{\partial t} A_2 = -i \left[ \frac{\beta_{22}}{2} \frac{\partial^2}{\partial t^2} - \gamma_2 (|A_2|^2 + \kappa(\delta) |A_1|^2) \right] A_2 + \gamma_2 \eta(\delta) |A_1|^2 A_2, \quad (2b)$$

$$\kappa(\delta) = (2 - \alpha) + \frac{\alpha}{1 + \delta^2 \tau^2}; \quad \eta(\delta) = \alpha \frac{\delta \tau}{1 + \delta^2 \tau^2}. \quad (2c)$$

In Eqs. (2a) and (2b)  $v_{gj}$  is the group velocity,  $\beta_{2j}$  is the GVD coefficient, and  $\gamma_j = n_2 \omega_j / (cA_{\text{eff}})$  is the nonlinear coefficient for the pump ( $j = 1$ ) and the signal ( $j = 2$ ) waves. The two parameters  $\kappa(\delta)$  and  $\eta(\delta)$ , defined in Eq. (2c), are the XPM coupling coefficient and the two-beam coupling (Raman) gain, respectively. It is worth noting that the “instantaneous” values  $\kappa = 2$

and  $\eta = 0$  are reached when at least one of the following conditions is fulfilled: (i) the nonlinearity is fast ( $\tau \ll 1/\delta$ ) or the probe frequency offset is small ( $\delta \ll 1/\tau$ ); (ii) the fractional contribution of the delayed nonlinearity is negligible  $\alpha \ll 1$ . In the case of a response time  $\tau \approx 1/\delta$ , the XPM coupling  $\kappa(\delta)$  has a

frequency dependence of Lorentzian type with an offset [see Eq. (2c)].

In our experiment, the pump power is orders of magnitude greater than the probe power  $|A_1|^2 \gg |A_2|^2$ ; hence, the XPM term in Eq. (2a) as well as the SPM term in Eq. (2b) can be neglected. The evolution equation for the pump wave (2a) becomes virtually decoupled from Eq. (2b) as far as the phase modulation terms are concerned:

$$\frac{\partial}{\partial z} A_1 + \frac{1}{v_{g1}} \frac{\partial}{\partial t} A_1 = -i \left( \frac{\beta_{21}}{2} \frac{\partial^2}{\partial t^2} - \gamma_1 |A_1|^2 \right) A_1 - \gamma_1 \eta(\delta) |A_2|^2 A_1, \quad (3a)$$

$$\frac{\partial}{\partial z} A_2 + \frac{1}{v_{g2}} \frac{\partial}{\partial t} A_2 = -i \left[ \frac{\beta_{22}}{2} \frac{\partial^2}{\partial t^2} - \gamma_2 \kappa(\delta) |A_1|^2 \right] A_2 + \gamma_2 \eta(\delta) |A_1|^2 A_2. \quad (3b)$$

Under the conditions of our experiment in Allwave fiber ( $\beta_{21} < 0$ ,  $\beta_{22} < 0$ ), the linear stability analysis of Eq. (3a) predicts the development of modulation instability for the pump wave  $A_1$  for frequencies  $|\Omega| < \Omega_c = \sqrt{4\gamma_1 P_1 / |\beta_{21}|}$ , with maximum gain  $g_{\max} = 2\gamma_1 P_1$  at  $\Omega_{\max} = \Omega_c / \sqrt{2}$ . It is clear that the low-frequency part of the spontaneous Raman scattering, which spectrally coincides with the peak of the MI gain, acts as a seed for the MI. As a result of this interaction, an amplitude modulation develops and the cw pump wave breaks up into pulses [2]. In the Truewave fiber, the pump wave is stable since it propagates in the normal dispersion regime, near the zero-dispersion point. This results in a corresponding stability of the probe wave (dashed lines in Fig. 1). In the Allwave fiber, the probe wave becomes unstable (solid lines in Fig. 1) due to the interplay between anomalous GVD and time-dependent XPM. Its spectrum becomes broadened, with characteristic sidebands appearing around the central frequency  $\omega_2$ . We can estimate the rms broadening  $\Delta\omega$  using the following relation [11]:

$$(\Delta\omega)^2 = \langle \omega^2 \rangle - \langle \omega \rangle^2 = \frac{\int \omega^2 |\tilde{A}_2(\omega)|^2 d\omega}{\int |\tilde{A}_2(\omega)|^2 d\omega} - \left( \frac{\int \omega |\tilde{A}_2(\omega)|^2 d\omega}{\int |\tilde{A}_2(\omega)|^2 d\omega} \right)^2, \quad (4)$$

where  $\tilde{A}_2(\omega)$  is the Fourier image of the solution of Eq. (3b). For simplicity, we neglect the Raman gain/loss terms in Eqs. (3a) and (3b) and assume that, due to MI, the pump wave has broken up into a train of picosecond pulses [2,12]. Provided XPM is the only nonlinear term in Eq. (3b), the solution for the probe wave with submegahertz initial spectral width  $\Delta\omega_0$  can be easily obtained:

$$A_2(L, t) = A_0 e^{-(\Delta\omega_0)^2 t^2} \exp(i\phi_m e^{-(t^2/a^2)}), \quad (5)$$

where  $a$  is the pump pulse duration [12] and  $\phi_m =$

$\gamma_2 \kappa(\delta) P_0 L$  is the maximum value of the nonlinear phase, acquired after an interaction length  $L$ . After substitution of Eq. (5) in Eq. (4), and taking into account that  $a\Delta\omega_0 \ll 1$ , we get:

$$\Delta(\delta) = \frac{1}{2} \Delta\omega = \frac{1}{2} \sqrt{\frac{\Delta\omega_0}{a}} \phi_m \sim \kappa(\delta). \quad (6)$$

Equation (6) provides the important relationship between the sideband frequency shift  $\Delta$  and the pump-probe frequency separation  $\delta$  observed in Fig. 1. According to the definition of the two-beam coupling coefficient  $\kappa(\delta)$  [see Eq. (2c)], this dependence has a Lorentzian shape. Its width is solely determined by the relaxation time  $\tau$  of the Raman nonlinearity. Hence, from a measurement of the frequency dependence of the sideband frequency shift  $\Delta(\delta)$ , one can deduce a value for the relaxation time  $\tau$ .

In Fig. 2, the measured blue sideband frequency shift  $\Delta$  is shown with solid squares for different values of the probe frequency offset  $\delta$ . For all data points in Fig. 2 both pump and probe powers are kept constant. It is seen that the Raman gain around  $\delta = 440 \text{ cm}^{-1}$  does not influence the trend in the frequency dependence of  $\Delta$ . Its effect simply manifests itself in the amplification of the weak sidebands, which otherwise might not be observable. We are therefore able to detect and measure the broadening only in the region of sufficient Raman gain ( $150\text{--}600 \text{ cm}^{-1}$ ). The best Lorentzian fit through the data points converges with a value  $\tau = 27(1) \text{ fs}$  for the relaxation time of the nonlinearity. Fitting the results from several independent measurements reproducibly yields the same value for  $\tau$ . The residuals from the fitting procedure (shown in the lower part of Fig. 2) are found to be evenly distributed throughout the whole frequency range, thus confirming the validity of Eq. (6). It is

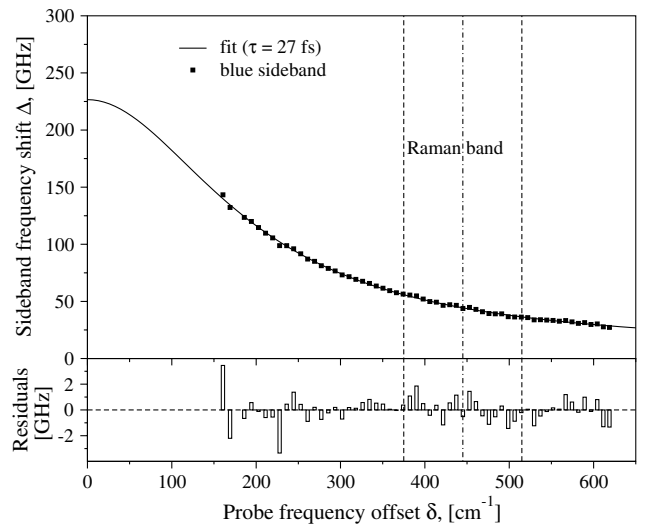


FIG. 2. Frequency dependence of the spectral broadening of the probe wave in forward pumped Raman amplifier in 25 km Allwave fiber. The solid line represents the best fit using Eq. (6).

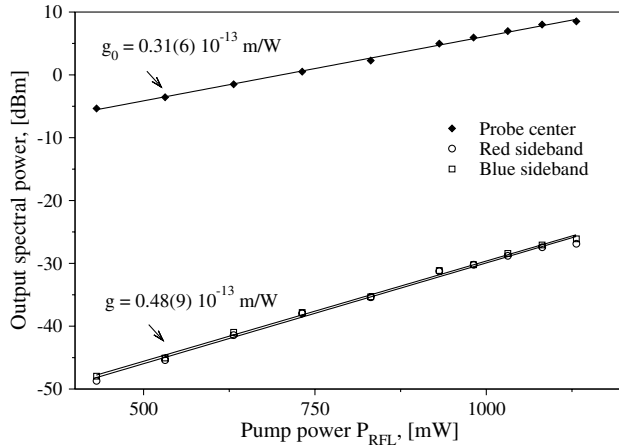


FIG. 3. Spectral power distribution at the output of 25 km Allwave fiber for different pump power levels at  $\delta = 430 \text{ cm}^{-1}$ .

important to note that a precise value for the relaxation time of the nuclear part of  $\chi^{(3)}$  in silica fibers has thus been experimentally determined through an interaction involving cw beams only. To our knowledge, this is the first direct measurement of this important material parameter. Values of the order of 30 fs have been assumed in numerical experiments [8] and have been shown to describe adequately the transient Raman scattering process. In a recent experimental study of Raman amplification in photonic crystal fibers, the presence of sidebands similar to those discussed in this Letter is evident in Fig. 3 of Ref. [13], but has not been explained.

In Fig. 3, the measured spectral powers for the probe (solid diamonds), the red (open circles), and the blue (open squares) sidebands for different pump powers  $P_{\text{RFL}}$  are presented. The probe frequency offset  $\delta = 430 \text{ cm}^{-1}$  was chosen in order to obtain both sufficient Raman gain and a large sideband frequency shift. All three amplification curves are seen to be purely exponential. From the slopes of the linear fits (in the semilogarithmic plot) the gain parameter for each amplification process can be extracted. The sidebands are found to experience higher gain than the central probe frequency. This fact provides clear evidence for the presence of MI gain transferred from the pump onto the signal wave via XPM and justifies the assumptions made in the theoretical treatment.

We have analyzed the development MI for two beams in noninstantaneous nonlinear media. The experimental

evidence obtained enables us to conclude that the observed instability is not simply due to the instantaneous interplay between XPM and GVD, but also involves the two-beam coupling resulting from the finite relaxation time of the Raman part of  $\chi^{(3)}$  in silica. From the analysis of the experimental data, we were able to extract an accurate value [ $\tau = 27(1)$  fs] for the lifetime of the optical phonons in silica. This type of experiment can be successfully used for the measurement of  $\tau$  in other materials with anomalous dispersion for both the pump and the probe waves. The spectral broadening observed is in the range of 20–150 GHz and may introduce inter-channel cross talk and deteriorate the performance of distributed Raman amplifiers. We have found that the effect is inhibited in counterpropagating pump geometry. The case of spatial MI in noninstantaneous nonlinear media has recently been analyzed in Ref. [14].

This work was supported by the National Science Foundation, Grant No. NSF DMR 9974031.

- 
- [1] K. Tai, A. Hasegawa, and A. Tomita, *Phys. Rev. Lett.* **56**, 135 (1986).
  - [2] A. S. Gouveia-Neto, M. E. Faldon, and J. R. Taylor, *Opt. Lett.* **13**, 1029 (1988).
  - [3] A. S. Gouveia-Neto, *J. Lightwave Technol.* **10**, 1536 (1992).
  - [4] G. P. Agrawal, *Phys. Rev. Lett.* **59**, 880 (1987).
  - [5] G. P. Agrawal, P. L. Baldek, and R. R. Alfano, *Phys. Rev. A* **39**, 3406 (1989).
  - [6] Y. Silberberg and I. Bar-Joseph, *J. Opt. Soc. Am. B* **1**, 662 (1984).
  - [7] J. J. Refi, *Bell Labs Tech. J.* **4**, 246 (1999).
  - [8] K. J. Blow and D. Wood, *IEEE J. Quantum Electron.* **25**, 2665 (1989).
  - [9] R. H. Stolen, J. P. Gordon, W. J. Tomlinson, and H. A. Haus, *J. Opt. Soc. Am. B* **6**, 1159 (1989).
  - [10] G. P. Agrawal, *Nonlinear Fiber Optics* (Academic, New York, 1989).
  - [11] S. C. Pinault and M. J. Potasek, *J. Opt. Soc. Am. B* **2**, 1318 (1985).
  - [12] N. N. Akhmedieva, V. M. Eleonskiĭ, and N. E. Kulagin, *Sov. Phys. JETP* **62**, 894 (1985).
  - [13] Z. Yusoff, J. H. Lee, W. Belardi, T. M. Monro, P. C. Teh, and D. J. Richardson, *Opt. Lett.* **27**, 424 (2002).
  - [14] M.-F. Shih, C.-C. Jeng, F.-W. Sheu, and C.-Y. Lin, *Phys. Rev. Lett.* **88**, 133902 (2002).